



Article

Freeze-Thaw Performance Characterization and Leachability of Potassium-Based Geopolymer Concrete

Peiman Azarsa and Rishi Gupta *

Civil Engineering Department, University of Victoria, Victoria, BC V8P-5C2, Canada; azarsap@uvic.ca

* Correspondence: guptar@uvic.ca; Tel.: +1-250-721-7033

Received: 28 March 2020; Accepted: 23 April 2020; Published: 27 April 2020



Abstract: It is well known that concrete is one of the most widely used construction materials in the world, and cement as its key constituent is partly responsible for global Carbon Dioxide (CO₂) emission. Due to these reasons, high strength concrete with lower CO₂ emission, and concrete with lower reliance on natural resources is increasingly popular. Geopolymer Concrete (GPC), due to its capability to minimize the consumption of natural resources, has attracted the attention of researchers. In cold regions, frost action is one of the primary GPC deterioration mechanisms requiring huge expenditures for repair and maintenance. In this regard, two types of GPC (fly-ash based GPC and bottom-ash based GPC) were exposed to the harsh freeze-thaw conditions using a standard test method. The dynamic elastic modulus of both types of GPC was determined using a Non-Destructive Test (NDT) method called Resonant Frequency Test (RFT). The results of RFT after exposing to 300 freeze-thaw cycles showed that bottom-ash based GPC has better freeze-thaw resistance than fly-ash based GPC. Moreover, in this study, the leachability of bottom-ash based GPC was also investigated to trace the heavy metals (including Si, Al, Na, Cr, Cu, Hg) using Toxicity Characteristic Leaching Procedure (TCLP) test. The results of the TCLP test showed that all of the heavy metals could be effectively immobilized into the geopolymer paste.

Keywords: geopolymer concrete; fly-ash; bottom-ash; freeze-thaw; leachability; non-destructive test; TCLP; RFT

1. Introduction

Fly-ash and bottom-ash are by-products of the combustion of pulverized coal in thermal power plants. These by-products are pozzolans and typically consist of Silicon Dioxide (SiO₂), Aluminum Oxide (Al₂O₃) and Iron Oxide (Fe₂O₃) [1]. It is projected by Miller et al. [2] that coal production will increase up to 1000 million tons annually by 2040. So, due to the environmental regulations, utilization of by-products such as fly-ash and bottom-ash in different applications must be provided to protect natural resources and avoid landfill disposal of ashes. Although, broadly speaking, the use of by-products in various industries leads to a cleaner environment, the Environmental Protection Agency [3] reported that by-products can pollute groundwater and can increase a person's health risk to incurable diseases. So, besides creating a durable concrete made using by-products, it is worthwhile to assess the environmental impact of concrete.

Ordinary Portland Concrete (OPC) is one of the most used construction materials all over the world due to its high durability, high mechanical properties and long service life. However, the production of cement as a main constituent of OPC requires energy that leads to the generation of Carbon Dioxide (CO₂). According to the Portland Cement Association (PCA), 1000 kg of Portland Cement Production releases 927 kg of CO₂ into the atmosphere [4]. Hence, to alleviate this impact on

the atmosphere, it is critical to reduce the use of Portland cement in the concrete by replacing it with other pozzolanic materials such as fly-ash, slag and bottom-ash.

Due to the issues mentioned above, scientists have been trying to use waste materials such as fly-ash to make durable concrete. However, the use of bottom-ash to produce concrete is not widely reported in the literature. French scientist Joseph Davidovits initially found one such concept, that of the "Geopolymer". Then, slag-based geopolymer cement was made in the 1980s [5]. Subsequently, in 1997, based on the obtained results for slag-based geopolymer cement, Silverstrim et al. [6], Van Jaarsveld and Van Deventer et al. [7] created an inorganic polymer concrete called Geopolymer Concrete (GPC). GPC is produced by reacting aluminate and silicate bearing materials with a caustic activator [8]. Since then, numerous works have reported on the development of Sodium-based (Na-based) GPC durability [9–12]. However, there are only limited studies conducted on the development of mix design, durability and service life of Potassium-based (K-based) GPC made by the combination of bottom-ash and fly-ash. Habert et al. [13] compared the environmental impact of GPC made by two types of by-products (fly-ash and slag), metakaolin and Ordinary Portland Concrete (OPC) using the Life Cycle Assessment (LCA) methodology. The results confirmed that GPC has a lower environmental impact in terms of emission of CO₂.

Freeze-thaw damage is a potentially critical deterioration mechanism that occurs not only in cement-based concrete but also in GPC structures. The reason for the deterioration of GPC in a cold condition is the water in cracks/capillary pores. The water in the cracks/capillary pores converts into ice when the material was exposed to the freeze-thaw cycles, where this issue leads to the internal expansion stress in the paste. This expansion stress causes internal micro-cracks. Continuously, an increase of freeze-thaw cycles leads to an extension of micro-cracks. Fu et al. [14] studied the freeze-thaw resistance of Na-based alkali-activated slag concrete. Six specimens of five mix proportions were cast and tested to measure the freeze-thaw resistance of alkali-activated slag concrete. Mass and Relative Dynamic Modulus of Elasticity (RDME) of each sample were measured after 25 freeze-thaw cycles. The result of the freeze-thaw test showed that RDME and mass of all mix proportions decrease about 10% and less than 1% after 300 cycles of freeze-thaw respectively. The authors also developed damage mechanics-based models using RDME. The authors reported that attenuation and power function models are more suited to accumulative and exponential damage models respectively.

This paper deals with the leachability of heavy metals of GPC. Basically, the potential leaching of heavy metals into the groundwater is a crucial concern with the use of by-products as a constituent of GPC, especially once the by-products are mixed with chemical materials such as Potassium Hydroxide (KOH) and Potassium Silicate (K₂O₃Si). Thang et al. [15] investigated the leachability of hazardous metals including Copper, Cadmium, Lead, Iron and Chromium of fly-ash based and red-mud-based geopolymer. Nine mix proportions were made to use Inductively Coupled Plasma- Atomic Emission Spectrometry (ICP-AES) at a pH of 7 to characterize the heavy metals in the geopolymer. The authors reported that raw materials leached a high amount of Lead, Palladium, Chromium and other hazardous metals. However, at a pH of 7, the level of leached metals from geopolymer materials was within the range specified by the European Standard. It is also found that geopolymer materials had lower concentrations than their constituent raw materials (fly-ash and red-mud). Arioiz et al. [16] studied the leachability of fly-ash based geopolymer paste cured at different temperatures, including 40 °C, 80 °C and 120 °C for 6, 15 and 24 h. The hazardous metals including Arsenic, Lead, Chromium, Cadmium and Mercury were characterized using Toxicity Characteristic Leaching Procedure (TCLP) test for samples and ICP-AES for solutions extracted from GPC and fly-ash. The results of the TCLP test showed that fly-ash has higher heavy metals concentration than geopolymer paste. Moreover, the higher concentration of Arsenic and Mercury were measured in the solution of the samples cured at 120 °C for 15 and 24 h.

2. Research Significance

First of all, ample studies on the durability and service life of Na-based GPC have been reported. However, limited studies have been reported on the mechanical properties of K-based GPC. Moreover,

it is reported that bottom-ash has similar physical, chemical and mechanical properties to fly-ash [17]. Since the use of bottom ash is relatively limited, dealing with this industrial material is now posing to be one of the most significant challenges in recent years. So, in the current study, attempts have been made to produce an appropriate mix proportion for K-based GPC made by a combination of 50% fly-ash and 50% bottom-ash (here noted as bottom-ash based GPC for further descriptions). K-based GPC synthesized only with fly-ash was also produced to compare its freeze-thaw resistance with bottom-ash based GPC.

Freeze-thaw delamination and heavy metals leaching are amongst the most persistent concerns of material in a frozen condition. Basically, aggressive environments damage the structure of GPC and consequently decrease their life span. Since there are limited studies that have reported on examination of the durability of K-based GPC, it is important to investigate the freeze-thaw resistance and leachability of K-based GPC synthesized by both fly-ash and bottom-ash.

Regarding freeze-thaw resistance properties, numerous predictive models were proposed for Na-based GPC [9,18,19]. Hongfa et al. [20] proposed a damage model for cement-based concrete. While, authors could not find any empirical model for K-based GPC, this model was used for K-based GPC in the current study. Moreover, the damage variable of K-based GPC was calculated and compared with other research studies to find the applicability of this freeze-thaw resistance model for by-products-based GPC [21,22].

3. Experimental Work

3.1. Precursors

Both fly-ash and bottom-ash were procured from Lafarge Inc. in Vancouver, Canada. According to ASTM C618 [23], the term fly-ash is divided into three categories (N, F, C). Class F was selected for the present study as it is a pozzolanic material and is useful for developing a durable GPC. Bottom-ash used in the current study had coarser particles than fly-ash. So, bottom-ash was sieved (#1.18 mm) to remove bigger size particles to increase the surface area of particles to achieve reasonable strength. The chemical elements obtained from the X-Ray Diffraction (XRD) test measured by Lafarge Inc. (due to the cost prohibitive nature of this test) are indicated in Table 1. It should be mentioned that the values of Na₂O, K₂O, TiO₂, P₂O₃, Mn₂O₃ of fly-ash are not measured by are the main components of both fly-ash and bottom-ash. The specific gravity of fly-ash and bottom-ash was 2.5 and 2.3 respectively.

Table 1. Chemical Compositions of fly-ash and bottom-ash.

Properties	Source: Lafarge Inc.'s Report	
	Fly-Ash (%)	Bottom-Ash (%)
SiO ₂	47.1	60.11
Al ₂ O ₃	17.4	14.35
Fe ₂ O ₃	5.7	5.92
CaO	14	10.40
MgO	5.4	4.49
SO ₃	0.8	0.10
LOI	0.19	0.00
Na ₂ O	N/A	2.232
K ₂ O	N/A	1.766
TiO ₂	N/A	0.892
P ₂ O ₅	N/A	0.200
Mn ₂ O ₃	N/A	0.093

Basically, a combination of alkali solution and soluble silicate is needed to produce GPC with desire durability. Since the durability of K-based GPC has only been reported by a few researchers [24,25], the combination of KOH and K₂SiO₃ was used in the present study because at elevated temperature

(higher than 30 °C, GPC made by K-based is more steady than Na-based GPC in terms of mechanical properties including compressive strength [26]. KOH flakes obtained from Sigma-Aldrich Private Ltd. (St. Louis, MO, USA), and K_2SiO_3 powder (AgSil 16) obtained from PQ Corporation (USA) were used in this study. Chemical elements of K_2SiO_3 obtained from the Material Safety Data Sheets (MSDS) of the product are shown in Table 2. The specific gravity of KOH and K_2SiO_3 was 1.45 and 1.26, respectively.

Table 2. Chemical composition of K_2SiO_3 .

Compound	K_2O	SiO_2	H_2O
%W/W	32.4%	52.8%	14.8%

Microstructural Study of Fly-Ash and Bottom-Ash

The Scanning Electron Microscopy (SEM) of fly-ash and bottom-ash was investigated using Hitachi S-4800 (Chiyoda, Tokyo, Japan) at the Advance Microscopic Facility (AMF) of the University of Victoria. The SEM operated at an accelerating voltage of 15 kV. Both fly-ash and bottom-ash were analyzed under 16.0 mm × 900 magnification.

The SEM images of both fly-ash and bottom-ash are presented in Figure 1i,ii. Figure 1i shows that the fly-ash particles are spherical in shape and hence known as cenospheres (perfectly round smooth and intact) with the presence of a few irregular particles. Figure 1ii shows the bottom-ash particles that are larger in size and sub-angular to angular in shape. It also can be seen that bottom-ash particles are porous with tiny pores visible in Figure 1. This porous nature of bottom-ash causes bottom-ash to absorb more water than fly-ash [27]. This needs to be properly accounted for when using bottom-ash in GPC production since excess water might have a negative impact on the GPC properties.

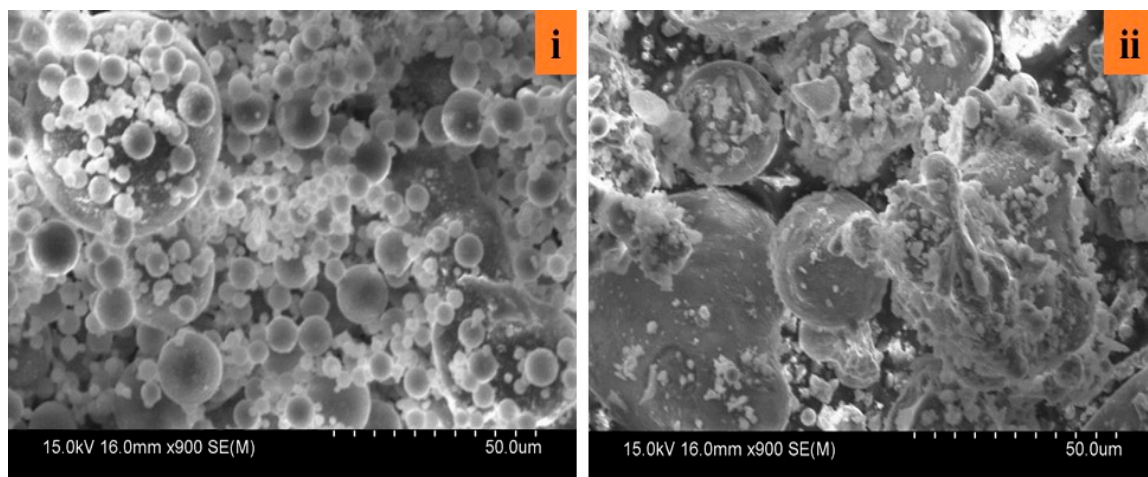


Figure 1. SEM images of fly-ash (i) and bottom-ash (ii).

3.2. Aggregates

Naturally available fine aggregate from Sechelt pit in B.C., Canada was used for the experimental work. Moisture content was measured by the change in weight of sample after keeping the sample for 24 h in an oven at 100 °C. The calculated moisture content was 4.10%. The fineness modulus, specific gravity and absorption of fine aggregate were 2.60, 2.65 and 0.79, respectively in accordance with ASTM C127 [28].

Coarse aggregate was also sourced from the Sechelt pit. The nominal size of the coarse aggregate was 12.5 mm. Calculated specific gravity, absorption and moisture content of coarse aggregate were 2.69, 0.69 and 1.39%, respectively in accordance with ASTM C127 [28]. The particle size distribution of coarse and fine aggregates was measured (shown in Figure 2) in accordance with ASTM C33 [29].

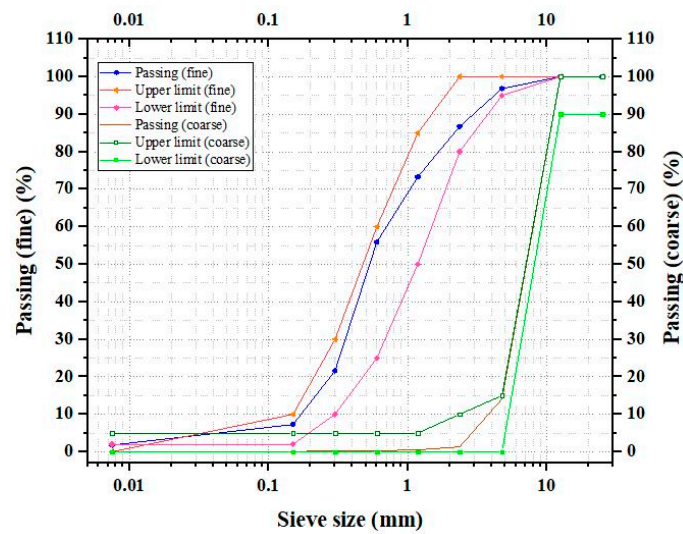


Figure 2. Aggregates size distribution.

3.3. Mix Design and Specimen Preparation of GPC

The mix proportion of GPC shown in Table 3 was derived after extensive initial trial experiments performed in the Facility for Innovative Materials and Infrastructure Monitoring (FIMIM) of the University of Victoria, Canada by the authors [12,30,31]. The KOH solution, with a concentration of 12 Molar (M), was prepared by dissolving KOH flakes in water. The KOH and K_2SiO_3 were mixed to prepare alkali activator solution in accordance with the mix design, provided in Table 3, 24 h before the casting day. The alkali activator ratio (K_2SiO_3/KOH) and a mass ratio of fly-ash to bottom-ash were considered to be 1.5 and 50:50 respectively to achieve a target strength of 35 MPa. This target strength was used as it is prescribed for numerous applications in practice.

Table 3. Mix Design.

Material	Bottom-Ash Based GPC (Kg/m ³)	Fly-Ash Based GPC (Kg/m ³)	Specific Gravity
Fly ash	194	388	2.5
Bottom ash	194	0	2.3
Coarse aggregates	1170	1170	2.69
Sand	630	630	2.60
KOH (12M)	85.16	85.16	1.45
K_2SiO_3	125.74	125.74	1.26
Extra Water	38.71	38.71	1
Air Entrained Admixture	1.5	1.5	1.03
Total	2439.11	2439.11	14.83

First, the alkali solution was prepared a day before casting day, as suggested by Davidovits [8]. Then GPC samples were produced in accordance with ASTM C192/C192M-15 [32] and ASTM C39/C39M-15 [33]. In order to produce GPC, dry materials were mixed in a concrete drum mixer for 1 min. Alkali solution was then added to the dry materials and was mixed for 3 min followed by a 3 min rest period. Finally, extra water (if the mixture was dry) was slowly added to the mixture for 2 min of final mixing. After mixing, GPC specimens were cast in molds (100 × 200 mm) for compressive test. Then, the Gilson vibrator table with a frequency of 60 Hz was used to discharge air bubbles to the surface, and for consolidating the specimens.

3.4. Curing of GPC Samples

Several efforts have been made for characterizing the influence of curing environments on different properties of Na-based GPC [34–36]. In previous studies performed by current authors [12,30,31] three methods of curing (ambient, steam and dry curing) were selected to accelerate the curing of K-based GPC and obtain higher compressive strength. So, in total, 54 cylindrical GPC samples (100 × 200 mm) were cured using the methods mentioned above. According to the results, steam-cured GPC samples showed greater compressive strength at temperature of 80 °C for 24 h. So, the steam curing method and temperature of 80 °C were used to cure fly-ash based and bottom-ash based GPC for this study.

Generally, for the steam curing method, after 24 h of ambient curing (approximate relative humidity range of 45% to 70% and approximate temperature range of 5 °C to 15 °C), the samples were left in a container surrounded by water. The container was packed tightly to prevent excessive evaporation during the curing process. The container was then put into the oven at a temperature of 80 °C. Lastly, the samples were removed from the oven, demolded, and was followed by 28 days of ambient curing. More details about the curing regime used are available in prior studies [12,30,31].

4. Methodology

Figure 3 shows the scope of work of this study. In this study, first of all, attempts have been made to produce bottom-ash based GPC and fly-ash based GPC using the steam curing method (at a temperature of 80 °C). After that, cylindrical bottom-ash based GPC and fly-ash based GPC specimens were made to measure their compressive strength. The freeze-thaw resistance, resonant frequency and leachability of bottom-ash based and fly-ash based beams were then tested using the Non-Destructive Test (NDT). Eventually, a comparative study was made between concrete parameter, compressive strength and number of cycles. It should be noted that the leachability of bottom-ash based GPC was separately studied using the TCLP test.

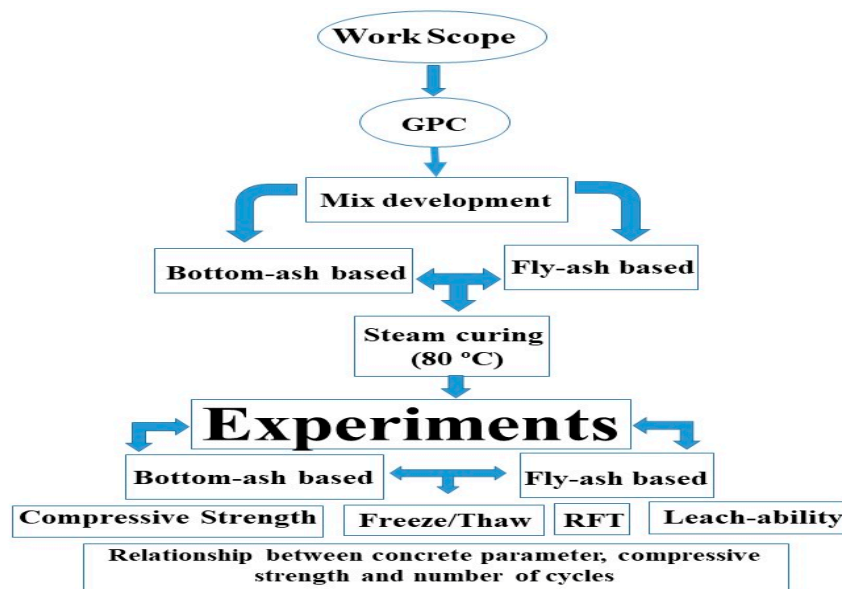


Figure 3. The work scope of the current study.

4.1. Compressive Strength

The steam-cured fly-ash based and bottom-ash based GPC samples (100 mm diameter and 200 mm height) were tested at the age of 28 days in accordance with ASTM C39/C39M-15 [33] using Forney compression testing machine model #AD 650.

4.2. Freeze-Thaw Test

In order to verify the durability of GPC under cold weather conditions, the freeze-thaw test was performed. Six GPC prisms (76 × 102 × 406 mm) were exposed to 300 freeze-thaw cycles, with temperature operating range from −17.8 °C to +4.4 °C and a humidity range from 10% to 95% in accordance with ASTM C666 [37]. Procedure “A” was selected in this study which arranges rapid freezing and thawing in water. After every 30 freeze-thaw cycles, samples were pulled off from the freeze-thaw cabinet to measure their mass loss, RDME and leaching.

4.3. Dynamic Elastic Modulus

One of the objectives of this research was to calculate the RDME using an NDT called Resonant Frequency Test (RFT)/Resonant Frequency Gauge (RTG). Figure 4 shows the components of the RFT/RTG device used for this study. Firstly, an accelerometer, with a frequency response measurement range of 20,000 Hz, was attached to the GPC surface using adhesive grease. After attaching the accelerometer and positioning GPC samples to the required mode of testing, a standard ball tip hammer weighing 110 ± 2 g with a tip diameter of 10 mm, is used to strike the surface at precise locations on the samples being tested. The achieved time domain signal was amplified and passed through BNC connection/cable. Finally, Olson instruments’ RTG software records/shows the resonant frequency. ASTM C666 [37] suggested the following equation to calculate the RDME:

$$P_c = \left(\frac{n_1^2}{n^2} \right) \times 100 \tag{1}$$

where:

P_c = RDME, %.

n = fundamental transverse frequency at 0 freeze-thaw cycles.

n_1 = fundamental transverse frequency after ‘n’ freeze-thaw cycles.

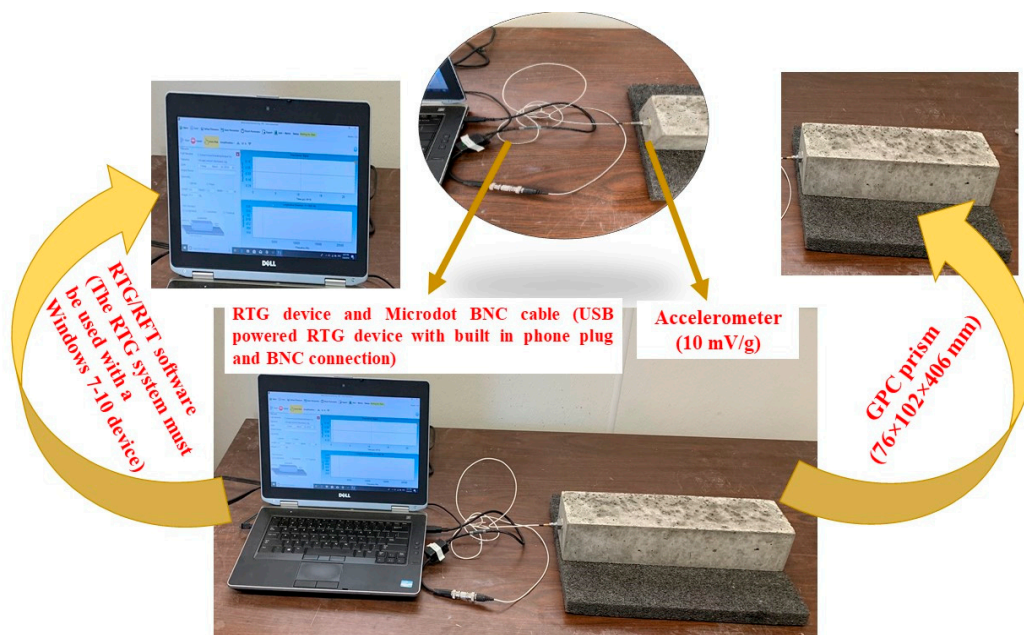


Figure 4. Resonant Frequency Test (RFT)/Resonant Frequency Gauge (RTG) Device.

5. Freeze-Thaw Damage Model

Hongfa et al. [20] used Aas-Jakobsen's [38] S-N equation (Equation (2)) and proposed a model (Equation (3)) for calculating the freeze-thaw damage of cement-based concrete in both the laboratory and real environmental conditions. According to their assumption, the freeze-thaw fatigue damage in concrete can be calculated as Equation (3):

$$S = \frac{\sigma'_{\max}}{f_t} = 1 - \beta (1 - R) \log N \quad (2)$$

$$D_n = 1 - \frac{0.6 \log N}{\log N - 0.4 \log(N - n)} = 1 - \frac{E_n}{E_0} \quad (3)$$

where:

D_n = freeze-thaw damage variable expressed as the RDME.

N = fatigue life of concrete exposed to freeze-thaw cycles.

n = number of freeze-thaw cycles.

E_0 = initial dynamic modulus of elasticity.

E_n = dynamic modulus of elasticity after 'n' freeze-thaw cycles.

β = concrete material parameter

They also determined the value of β under freeze-thaw conditions using Equation (4) and established a relationship between β and compressive strength.

$$\beta = \frac{D_n}{\log N} \quad (4)$$

In this study, the value of β of fly-ash based GPC and bottom-ash based GPC and other by-products-based GPC performed by Zhao et al. [21] and Mengxuan et al. [22] was calculated to find the applicability of Equation 4. Table 4 compares the mix proportions of other researchers [21,22] to the ones used in this study. Equations (3) and (4) were used to calculate the value of β of each mix proportion (shown in Table 4), and to establish the relationship between β , number of cycles and compressive strength of each mix proportion.

6. TCLP Test

Several materials are categorized as hazardous waste when they are dumped in landfills. GPC is considered as a toxic material due to the use of hazardous waste materials and chemical activators in its mixture. This is why it is vital to check its chemical metals leachability. In this study, the TCLP test was used to analyze the leaching of chemical metals from GPC. To study the environmental compatibility of K-based GPC made by 50% fly-ash and 50% bottom-ash, TCLP was performed as per USEPA 1311.

In this study, GPC was crushed to achieve a minimum of 100 g to characterize the chemical metals. Then, 5 g of GPC sample was mixed with 95 mL of distilled water to measure its pH level. After the determination of pH value, a proper extraction fluid was selected and was added to 100 g \pm 0.1 g of GPC sample (< 9.5 mm). The solution was placed in the extraction vessel and was rotated at 30 \pm 2 rpm for 18 \pm 2 hrs at ambient temperature (23 \pm 2 °C). At the end of the extraction period, the solution was transferred to the filter holder. The filtrate collected is called leachate.

Table 4. Comparison of mix proportions.

Sample	Mixture	Fly-ash	Slag	Cement	Sand	Gravel	Na ₂ SiO ₃	NaOH	Water	Water reducer	Curing	Si/Al	L/S
1	OPCC [21]	56 (kg/m ³)	56 (kg/m ³)	448 (kg/m ³)	626 (kg/m ³)	1022 (kg/m ³)	-	-	174.7 (kg/m ³)	2.5 (kg/m ³)	Standard	-	-
2	GPC-10 [21]	346.7 (kg/m ³)	38.5 (kg/m ³)	-	601.7 (kg/m ³)	1203.5 (kg/m ³)	165.7 (kg/m ³)	66.2 (kg/m ³)	-	-	80 °C	-	-
3	GPC-30 [21]	269.6 (kg/m ³)	115.6 (kg/m ³)	-	601.7 (kg/m ³)	1203.5 (kg/m ³)	165.7 (kg/m ³)	66.2 (kg/m ³)	-	-	Standard	-	-
4	GPC-50 [21]	192.6 (kg/m ³)	192.6 (kg/m ³)	-	601.7 (kg/m ³)	1203.5 (kg/m ³)	165.7 (kg/m ³)	66.2 (kg/m ³)	-	-	Standard	-	-
5	RMSFFA-SA2.0-NA0.6-RT-28D [22]	-	-	-	-	-	-	-	25%	25%	Room temp. (23 °C)	2.00 mol	0.53
6	RMSFFA-SA2.0-NA0.6-80C-28D [22]	-	-	-	-	-	-	-	25%	25%	80 °C	2.00 mol	0.53
7	Fly-ash based GPC (current study)					Available in Table 3							
8	Bottom-ash based GPC (current study)					Available in Table 3							

7. Results and Discussion

7.1. Physical Characteristics

The slump test was performed for the analysis of viscosity behavior of fly-ash based GPC and bottom-ash based GPC to investigate the workability, according to ASTM C143 [39]. The average slump value of fly-ash based GPC and bottom-ash based GPC was measured as 245 mm and 215 mm, respectively. The bottom-ash based GPC specimens showed lower workability than fly-ash based GPC specimens because according to the microscopic study of GPC, the smooth surface and rounded-shape of the fly-ash particles improve ball-bearing effect, which increase the workability [40]. Moreover, it can be seen from Table 3 that bottom ash has a lower specific gravity when compared to fly-ash. Hence, when the same weight of fly-ash per cubic meter of the material is replaced with bottom ash, there is more dry volume of the material, which may also be partly responsible for reducing the workability of the mix.

The average dry density of fly-ash based GPC and bottom-ash based GPC at 7 days was 2415 kg/m³ and 2422 kg/m³, respectively. The dry density of these two types of GPC increased as the age of the GPCs increased. The average dry density of fly-ash based GPC increased from 2415 kg/m³ to 2431 kg/m³ when age of samples increased from 7 days to 28 days with an overall increase of 0.66%. In contrast, the average dry density of bottom-ash based GPC increased from 2422 kg/m³ at 7 days to 2435 kg/m³ at 28 days with an overall increase of 0.53%. The authors attribute this slight difference in density to in-batch test variability.

It is well-known that the specific gravity of fly-ash and bottom-ash is comparable because these two materials have similar chemical compositions. Table 3 indicates that fly-ash has higher specific gravity compared to its counterpart bottom-ash. It is reported that cenospheres and poor gradation of particles degrade specific gravity of bottom-ash [41].

7.2. Compressive Strength of GPC

It is well-known that elevated curing temperature and duration are beneficial toward the acceleration of the polycondensation process. In previous studies performed by current authors, three methods of curing (ambient, steam and dry curing) were used to achieve higher compressive strength. A minimum of six specimens (100 × 200 mm) were cured at ambient, 30, 45, 60, 80 °C for 24 h and then kept at room temperature for 28 days. These samples were tested at the age of 28 days by using Forney compressive testing machine model #AD 650. However, steam-cured GPC at a temperature of 80 °C for 24 h following by 28 days of room temperature curing achieved higher average compressive strength (35 MPa). Based on the other studies on the microstructure of GPC [42,43], the steam curing method improves the dissolution rate of chemical species, such as Silicon Dioxide (SiO₂) and Aluminum Oxide (Al₂O₃), from mixture where the rate of geopolymerization increases. This finding can be attributed to the full and uniform internal curing of specimens. This finding is also in good-agreement with Yewale et al. [44], where the optimum compressive strength of steam-cured GPC was achieved at 80 °C. So, in the present study, GPC samples were steam-cured at 80 °C for subsequent experiments. However, it should be mentioned that GPC samples can be steam-cured at 60 °C for some applications and it may not be necessary to cure at high temperature such as 80 °C.

The same method and temperature (80 °C) were then used to produce fly-ash based GPC. A minimum of three fly-ash GPC cylinders were cast to find their average compressive strength at the age of 28 days. The compressive strength of fly-ash based GPC specimens was 32 MPa, 30 MPa and 32 MPa with an average of 31 MPa. It can be seen from the results of the compression test that the compressive strength of bottom-ash based GPC steam-cured at 80 °C is higher than fly-ash based GPC with a similar curing regime. Although several studies have reported that bottom-ash based GPC has lower compressive strength compared to fly-ash based GPC [27,45,46], it can be attributed to the higher porosity of bottom-ash [47]. However, it should be noted that the ratio of SiO₂/Al₂O₃ also affects the compressive strength of GPC [48,49]. This means that GPC made by waste ashes with a higher of SiO₂/Al₂O₃ ratio tend to develop higher compressive strength. In this study, the bottom-ash

had a higher $\text{SiO}_2/\text{Al}_2\text{O}_3$ ratio than fly-ash. This is why bottom-ash based GPC had higher compressive strength compared to fly-ash based GPC.

Generally, Na-based solution is mostly considered in various studies due to its low cost, availability, desired workability and durability. However, the K-based solution can also be used for high temperature applications [48,50–52]. According to Hounsi et al. [53], Na-based GPC gains lower compressive strength value than K-based GPC at the same alkali concentration of the current study (12 M). Hounsi et al. [53] attributed this phenomenon to the reduction of Si/Na ratio at a high concentration of sodium hydroxide (NaOH), where NaOH slows the polycondensation process and reduces the mechanical properties of Na-based GPC.

In previous studies performed by current authors, attempts have been made to cure the samples at ambient temperature. However, as aforementioned, the higher compressive strength is achieved at 80 °C. It is well known that only ambient temperature curing is a practical method in the construction field for GPC and to save energy. Hence, mixing calcium-based material such as cement with ashes is suggested to improve setting time, workability and durability of GPC cured at ambient temperature [54]. The microstructural investigation of fly-ash based GPC mixed with cement showed that the geopolymerization process is more likely as calcium alumino-silicate hydrate (C-A-S-H), which contributes to hardening and early strength gain of GPC mix with cement. Moreover, the enhanced strength of GPC mixed with cement is attributed to the generated heat during the geopolymerization process, where cement helps GPC to initiate condensation reaction at ambient temperature [35].

7.3. Freeze-Thaw Resistance

7.3.1. Mass Loss of Specimens during the Freeze-Thaw Process

The weight of GPC was taken every 30 cycles of freeze-thaw to calculate their mass loss. Figure 5 shows the average mass loss of six fly-ash based GPC and six bottom-ash based GPC up to 300 cycles of freeze-thaw. Fly-ash based GPC shows higher and rapid mass loss possibly because the specimens' structure failed at the early age of freeze-thaw cycles, and due to the poor bonding in the Interfacial Transition Zone (ITZ) which led to severe surface scaling. This finding is in good-agreement with the mass loss result of fly-ash based GPC-10 studied by Zhao et al. [21]. In contrast to fly-ash based GPC, the mass loss of bottom-ash based GPC was slow till 300 freeze-thaw cycles which indicates higher bonding strength of paste of bottom-ash based GPC.

7.3.2. RDME of Fly-Ash Based and Bottom-Ash Based GPC

Figure 6 indicates the average RDME reduction of six fly-ash based GPC and six bottom-ash based GPC over 300 cycles of freeze-thaw. As can be seen in Figure 6, bottom-ash based GPC exhibits higher RDME than fly-ash based GPC. The RDME of both types of GPCs dramatically dropped when cycles increased from 0 to 60. Authors attribute this RDME reduction to the existence of uncured by-product particles in the microstructure of GPC that caused GPC specimens to lose its microstructural strength at early freeze-thaw cycles [55].

It also can be seen that RDME loss of bottom-ash based GPC (13.4%) was higher than fly-ash based GPC (10.9%) until 60 cycles. However, RDME of fly-ash based GPC reduced intensely until 150 cycles (RDME \approx 60%). In this study, the freeze-thaw test for fly-ash based GPC was continued up to 300 cycles, even though according to ASTM C666 [37], the freeze-thaw testing procedure of specimen must be stopped when its RDME reaches 60% of the initial modulus. Since concrete is a heterogeneous material, the issue mentioned above might be due to the various factors such as the density and RDME of the main constituents (such as fly-ash and bottom-ash) and the characteristic of the ITZ which affect the elastic behavior of the composite [56]. Moreover, in general, the RDME of the fly-ash based matrix and bottom-ash matrix are determined by their porosity. So, the parameters determining the porosity of the matrix, such as geopolymerization process, curing conditions, AEA amount, etc., could be the other reasons for rapid RDME reduction of fly-ash based GPC.

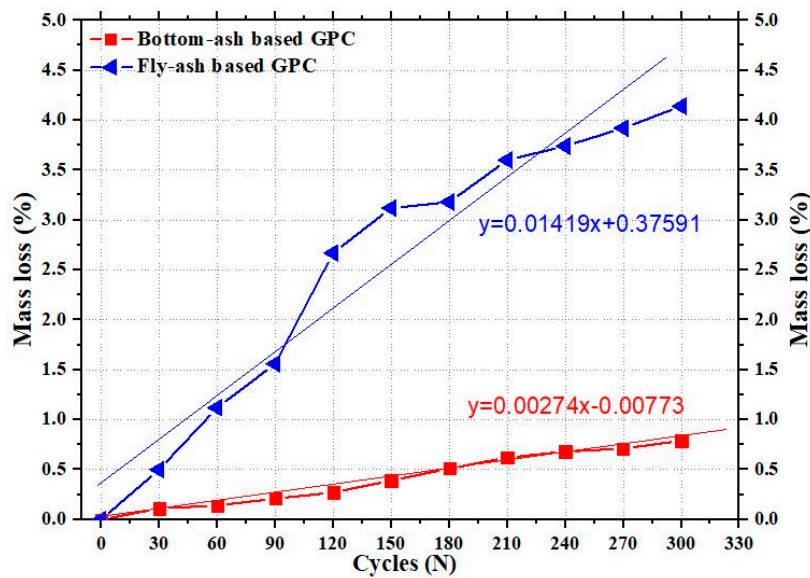


Figure 5. Average mass loss of fly-ash based Geopolymer Concrete (GPC) and bottom-ash based GPC over 300 cycles of freeze-thaw.

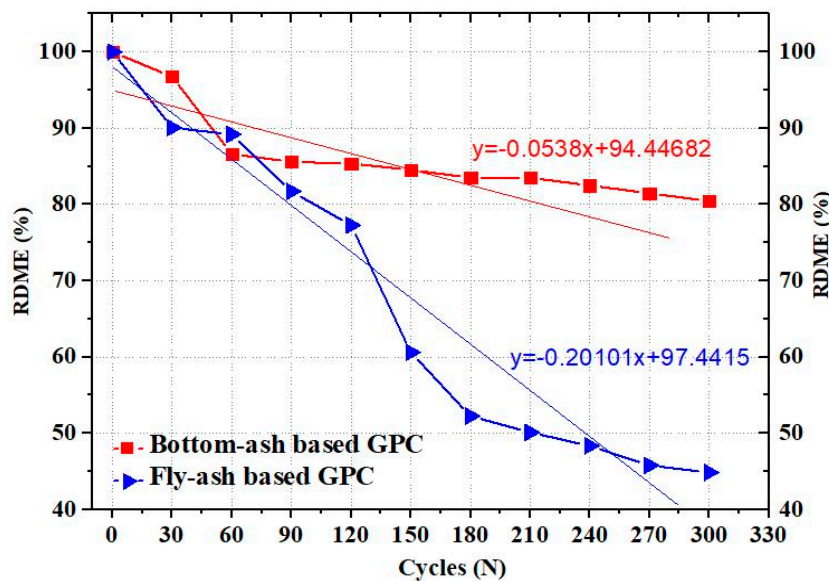


Figure 6. Average Relative Dynamic Modulus of Elasticity (RDME) reduction of fly-ash based GPC and bottom-ash based GPC vs. No. of cycles.

It is well-known that Air Entrained Admixture (AEA) provides more free spaces for the water to freeze. However, the pressure made by cryo (ice formation inside the air voids of GPC) can overcome the tensile strength of the matrix when these free spaces are overloaded with cryo. Consequently, this pressure creates micro-cracks in the ITZ and would reduce the ultimate strength of concrete. So, fly-ash based GPC can bear lower force when exposed to the freezing and thawing conditions since the initial compressive strength of fly-ash based GPC (~32 MPa) was lower than bottom-ash based GPC (~35 MPa).

7.4. Leachability of GPC

7.4.1. Laboratory Investigation of Bottom-Ash Based GPC

Identification of heavy metals and their leaching is one of the important factors that govern the utilization of GPC because of its influence on the environment. The toxicity of heavy metals depends

on their concentration rate in the environment. With the increasing concentration rate of heavy metals in the environment, these toxic hazardous metals can be accumulated in living tissues and cause irreparable events. So, the TCLP test was conducted for obtaining the essential data about main chemical elements such as Si, Al, Na and other hazardous metals such as Cr, Cu, Hg, etc. It should be mentioned that the TCLP test was only possible on one sample due to the cost prohibitive nature of this test. Bottom-ash based GPC was selected in this study because of its higher freeze-thaw resistance than fly-ash based GPC. The TCLP test was performed by the Maxxam Analytics lab, Victoria, Canada. Table 5 shows the pH of bottom-ash based GPC at three levels of extractions. The initial pH of the sample was 11.6 due to the existence of alkali constituents (K-based) in the bottom-ash based GPC mixture. To prepare the leaching/extraction fluid, 5.7 mL glacial acetic acid (CH₃CH₂OOH) was added to 500 mL reagent/distilled water. When reasonably mixed, the pH of this fluid was 4.96. Then, to perform the TCLP test, an amount of the proper leaching fluid equivalent to 20 times the mass of the specimen (20:1 liquid to solid ratio) was added to the extraction vessel of TCLP equipment. Then, the measured pH of leachate was 6.36.

Table 5. pH values of bottom-ash based GPC.

pH	-
Initial pH of sample	11.6
Final pH of leachate	6.36
pH of leaching fluid	4.96

The results of the TCLP test showed that all the heavy metals could be effectively immobilized into the geopolymeric paste. Figure 7 indicates that Ba, B and Fe have the highest leaching concentration and the rest of heavy metals have a concentration of less than 0.10 mg/L. Moreover, the obtained results showed that the concentration of all the heavy metals is below the regulatory level in accordance with USEPA 1311 and USEPA CFR. This could be attributed to the cations of heavy metals (such as Cu²⁺, Cd²⁺, Fe³⁺, Zn²⁺, Pb²⁺, and total Cr) that can participate in the balance of the negative charge of tetra-silicate ([SiO₄]⁴⁻) and potassium tetra-aluminate ([K⁺AlO₄]⁴⁻) [57,58]. So, bottom-ash based GPC showed low porosity, which could help immobilize all the heavy metals [59,60].

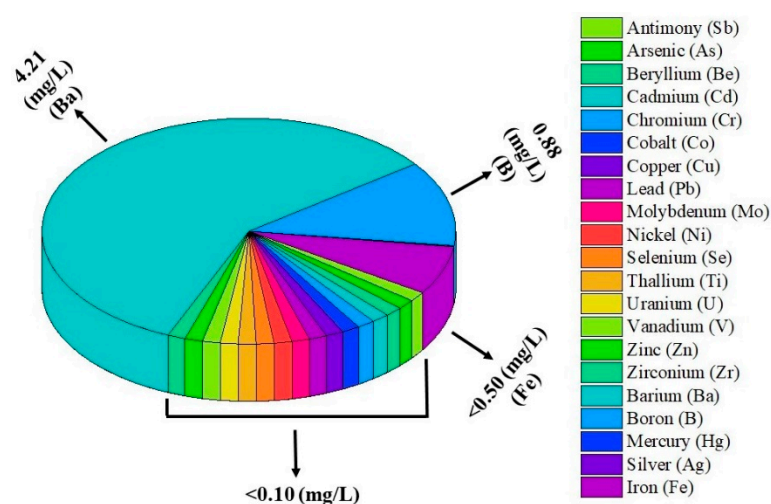


Figure 7. Toxicity Characteristic Leaching Procedure (TCLP) test results of bottom-ash based GPC.

7.4.2. Observational Study on Leachability of GPC during the Freeze-Thaw Process

In this study, the leachability of fly-ash-based GPC and bottom-ash based GPC was measured using a water testing method called HACH strips. The water sample was collected every 30 cycles

from the freeze-thaw cabinet to measure the leachability of fly-ash based GPC and bottom-ash based GPC. Since the trend of data for every 30 cycles was quite similar only results obtained from the last cycle (300 cycles) were analyzed and plotted in Figure 8. The leachability of both fly-ash based GPC and bottom-ash based GPC was constant over 300 cycles of freeze-thaw (Figure 8). This phenomenon shows that the geopolymerization process was fully completed, and all toxic metals were trapped in the paste. Moreover, heat-treatment improved the microstructure of the GPC specimens, decreased the porosity and decreased the leachability of the paste [61].

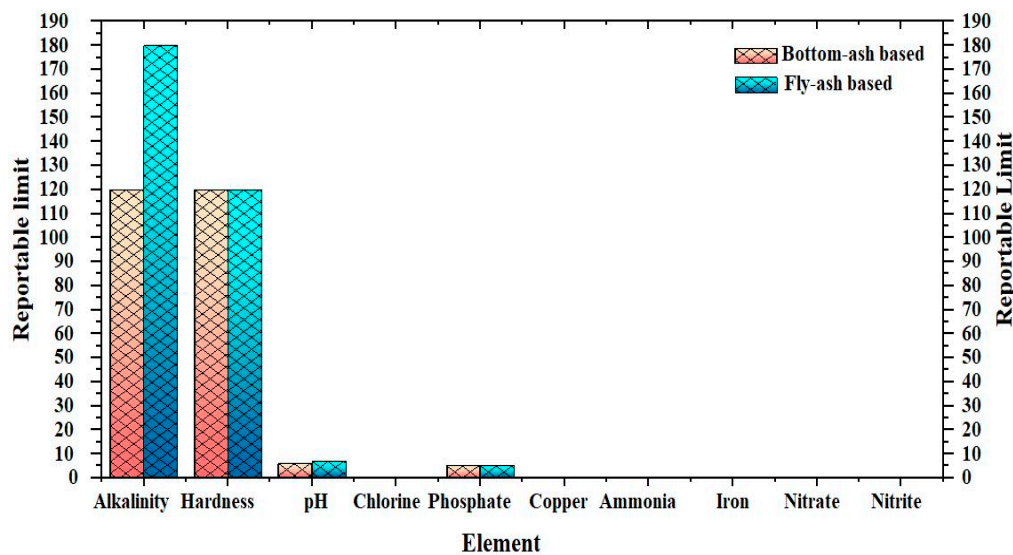


Figure 8. Leaching range of GPCs over 300 freeze-thaw cycles.

It also can be seen that the concentration of all the elements is almost in same range. However, fly-ash based GPC had more amount of alkalinity than bottom-ash based GPC, possibly due to poor geopolymerization of fly-ash based GPC compared to bottom-ash based GPC, which led to leaching of potassium from fly-ash based GPC.

7.5. The Relationship between β , Number of Cycles and Compressive Strength of GPC

Figure 9 shows calculated values of β for data obtained from Zhao et al. [21] and Mengxuan et al. [22] and compares with values of β of fly-ash based GPC and bottom-ash based GPC. The value of β for mix #1, 2, 3, 4, 5, 6, 7 and 8 is 0.19, 0.44, 0.22, 0.19, 0.27, 0.23, 0.18 and 0.16, respectively. According to Equation 4, the value of β is inversely proportional to the logarithmic function of N, which means a higher number of freeze-thaw cycles give a lower value of β . The results of the current experiment, shown in Figure 9, confirm the finding mentioned above that bottom-ash based GPC (mix #8) with a lower value of β has higher freeze-thaw resistance than fly-ash based GPC (mix #7). This finding is also applicable to the rest of the GPC samples. Moreover, it can be seen that the value of β for GPC samples with compressive strength less than 50 MPa decreased abruptly. While, β value of GPC samples with compressive strength higher than 50 MPa reduced gradually. Although the results of the current study are in good agreement with Hongfa et al. [20], the authors suggest that compressive strength of GPC should be considered in Hongfa et al.'s [20] equation because compressive strength is one of the key properties of GPC revealing internal bonding of paste. Therefore, a greater number of freeze-thaw cycles were achieved when GPC had higher bonding strength. This finding can be seen in Figure 9 where the value of β was varied when compressive strength increased (the value of compressive strength of mix #1, 3, 4 and 8 was higher than their β , while the compressive strength of mix #2, 5, 6 and 7 was lower than their β).

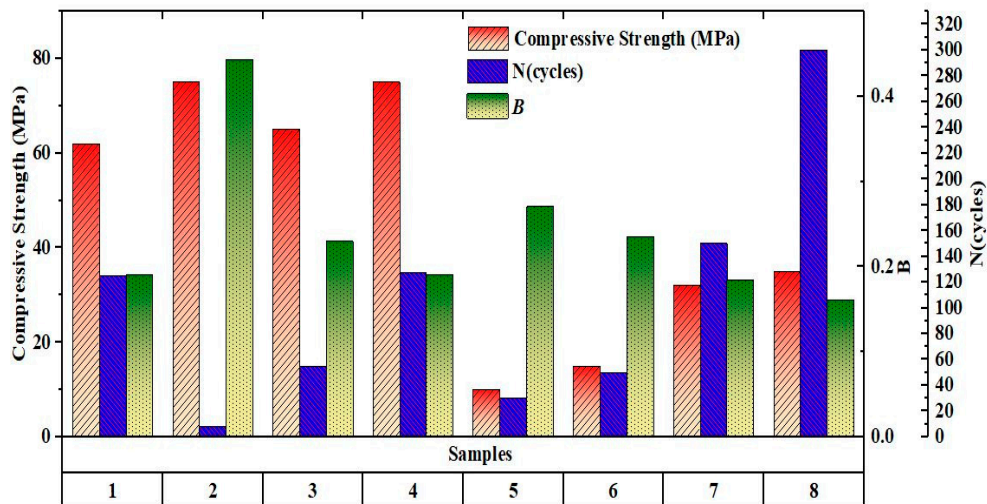


Figure 9. Value of β , compressive strength and number of cycles for different types of GPC.

8. Conclusions

In this study, the deterioration and mass loss produced in fly-ash based GPC and bottom-ash based GPC during 300 cycles of freeze-thaw were evaluated using RFT. Leachability of bottom-ash based GPC was also measured using the TCLP test to characterize the heavy metals. According to the obtained results:

- Bottom-ash based GPC indicated lower mass loss than fly-ash based GPC. Authors attributed the phenomenon mentioned above to the poor bonding of pastes in the ITZ in fly-ash based GPC.
- The resonant frequency of both types of GPC was measured after exposure to 300 freeze-thaw cycles with interval of 30 cycles. According to the results, bottom-ash based GPC showed better freeze-thaw resistance than fly-ash based GPC. It could be attributed to various parameters including geopolymerization process, curing conditions and the amount of AEA.
- Toxicity of heavy metals leaching from bottom-ash based GPC was measured using the TCLP test. The results showed that all the heavy metals including Si, Al, Na, Cr, Cu, Hg etc. were trapped and immobilized in the paste, and all of them were below the standard range of USEPA 1311 and USEPA CFR.
- A comparison between compressive strength, N and β of different types of by-products-based GPC was made. The experimental results showed that a higher number of freeze-thaw cycles give lower β . So, Bottom-ash based GPC with a higher number of cycles had lower β (0.1614) than fly-ash based GPC (0.1838). The authors also found that compressive strength should be accounted for in the proposed equation by Hongfa et al. [20].

Author Contributions: P.A. made different mix propositions and produced all the samples to find the higher compressive strength for these types of concrete. He also performed the compressive strength test, freeze-thaw test and resonant frequency test to investigate and estimate durability of fly-ash based and bottom-ash based GPC. R.G. provided the materials and shared knowledge on this subject. P.A. wrote the paper and R.G. revised it. All authors have read and agreed to the published version of the manuscript.

Funding: This research was funded by India Canada Research Centre of Excellence (IC-IMPACTS).

Acknowledgments: This research paper is made possible through the help and financial support from IC-IMPACTS. Authors also would like to thank all the staff in Civil Engineering department of University of Victoria.

Conflicts of Interest: The authors declare no conflict of interest.

References

1. Zimring, C.A.; Rathje, L. *Encyclopedia of Consumption and Waste: The Social Science of Garbage*, 2nd ed.; SAGE: New York, NY, USA, 2012.
2. Miller, B.G. The future role of coal. In *Clean Coal Engineering Technology*, 2nd ed.; Elsevier: Amsterdam, The Netherlands, 2017; ISBN 978-0-12-811365-3.
3. Environmental Protection Agency, Federal Registration, 17 April 2015. Available online: <https://www.federalregister.gov/documents/2015/04/17/20150-0257/hazardous-and-solid-waste-management-system-disposal-of-coal-combustion-residuals-from-electric> (accessed on 14 October 2015).
4. Marceau, M.; Nisbet, M.; Geem, M.V. *Life Cycle Inventory of Portland Cement Manufacture*; Portland Cement Association: Skokie, IL, USA, 2006.
5. Davidovits, J. Geopolymer cement: A review. *Geopolym. Sci. Tech.* **2013**, *21*, 1–11.
6. Silverstrim, T.; Rostami, H.; Larralde, J.; Samadi-Maybodi, A. Fly Ash Cementitious Material and Method of Making a Product. U.S. Patent 5,601,643, 11 February 1997.
7. Van Jaarsveld, J.G.S.; van Deventer, J.S.J.; Lorenzen, L. The potential use of geopolymeric materials to immobilize toxic metals: Part I. Theory and applications. *Miner. Eng.* **1997**, *7*, 659–669. [[CrossRef](#)]
8. Davidovits, J. *Geopolymer Chemistry and Application*, 4th ed.; Institut Geopolymere: Saint-Quentin, France, 2015.
9. Okoye, F.; Durgaprasad, J.; Singh, N.B. Fly ash/kaolin based geopolymer green concretes and their mechanical properties. *Data Brief.* **2015**, *5*, 739–744. [[CrossRef](#)] [[PubMed](#)]
10. Vora, P.R.; Dave, U. Parametric studies on compressive strength of geopolymer concrete. *Procedia Engineering* **2013**, *51*, 210–219. [[CrossRef](#)]
11. Shaikh, F.U.A. Mechanical and durability properties of fly ash geopolymer concrete containing recycled coarse aggregates. *Int. J. Sustain. Built Environ.* **2016**, *5*, 277–287. [[CrossRef](#)]
12. Gupta, R.; Rathod, H. Current state of K-based geopolymer cements cured at ambient temperature. *Emerg. Mater. Res.* **2015**, *4*, 125–129. [[CrossRef](#)]
13. Habert, G.; De Lacaillerie, J.B.D.E.; Roussel, N. An environmental evaluation of geopolymer based concrete production: Reviewing current research trends. *Clean. Prod.* **2011**, *11*, 1229–1238. [[CrossRef](#)]
14. Fu, Y.; Cai, L.; Wu, Y. Freeze–thaw cycle test and damage mechanics models of alkali-activated slag concrete. *Constr. Build. Mater.* **2011**, *25*, 3144–3148. [[CrossRef](#)]
15. Thang, N.H.; Ha, B.T.Q.; Ha, P.V.T.; Minh, D.Q.; Duc, H.M.; Quang, L.V. Leaching behavior and immobilization of heavy metals in geopolymer synthesized from red mud and fly ash. *Key Eng. Mater.* **2018**, *777*, 518–522.
16. Arioz, E.; Arioz, O.; Kockar, O.M. Leaching of F-type fly ash based geopolymers. *Procedia Eng.* **2012**, *42*, 1114–1120. [[CrossRef](#)]
17. Argiz, C.; Sanjuan, M.A.; Menedez, E. Coal bottom ash for Portland cement production. *Adv. Mater. Sci. Eng.* **2017**, *2017*, 7. [[CrossRef](#)]
18. Lee, W.-H.; Wang, J.-H.; Ding, Y.-C.; Cheng, T.-W. A study on the characteristics and microstructures of GGBS/FA based geopolymer paste and concrete. *Constr. Build. Mater.* **2019**, *211*, 807–819. [[CrossRef](#)]
19. Hamidi, M.R.; Man, Z.; Azizli, K.A. Concentration of NaOH and the effect on the properties of fly ash based geopolymer. *Procedia Eng.* **2016**, *148*, 189–193. [[CrossRef](#)]
20. Hongfa, Y.; Haoxia, M.; Kun, Y. An equation for determining freeze-thaw fatigue damage in concrete and a model for predicting the service life. *Constr. Build. Mater.* **2017**, *137*, 104–116.
21. Zhao, R.; Yuan, Y.; Cheng, Z.; Wen, T.; Li, J.; Li, F.; Ma, Z.J. Freeze-thaw resistance of class F fly ash-based geopolymer concrete. *Constr. Build. Mater.* **2019**, *222*, 474–483. [[CrossRef](#)]
22. Mengxuan, Z.; Zhang, G.; Htet, K.W.; Kwon, M.; Kwon, M.; Xu, Y.; Tao, M. Freeze-thaw durability of red mud slurry-class F fly ash-based geopolymer: Effect of curing conditions. *Constr. Build. Mater.* **2019**, *215*, 381–390.
23. ASTM C618. *Standard Specification for Coal Fly Ash and Raw or Calcined Natural Pozzolan for Use in Concrete*; ASTM: West Conshohocken, PA, USA, 2017.
24. Sakkas, K.; Panias, D.; Nomikos, P.P.; Sofiano, A.I. Potassium based geopolymer for passive fire protection of concrete tunnels linings. *Tunn. Undergr. Space Technol.* **2014**, *43*, 148–156. [[CrossRef](#)]
25. Hosan, A.; Haque, S.; Shaikh, F. Comparative study of sodium and potassium based fly-ash geopolymer at elevated temperature. In *Proceedings of the International Conference on Performance-based and Life-cycle Structural Engineering*, Brisbane, QLD, Australia, 9–11 December 2015.

26. Hosan, A.; Haque, S.; Shaikh, F. Compressive behaviour of sodium and potassium activators synthesized flyash geopolymer at elevated temperatures: A comparative study. *J. Build. Eng.* **2016**, *8*, 123–130. [[CrossRef](#)]
27. Haq, E.; Padmanabhan, S.K.; Licciulli, A. Synthesis and characteristics of fly ash and bottom ash based geopolymers—A comparative study. *Ceram. Int.* **2014**, *40*, 2965–2971. [[CrossRef](#)]
28. American Society for Testing and Materials. *Standard Test Method for Relative Density (Specific Gravity) and Absorption of Coarse Aggregate*; ASTM C127/C127M; American Society for Testing and Materials: West Conshohocken, PA, USA, 2015.
29. American Society for Testing and Materials. *Standard Specification for Concrete Aggregates*; ASTM C33/C33M; American Society for Testing and Materials: West Conshohocken, PA, USA, 2015.
30. Belforti, F.; Azarsa, P.; Gupta, R.; Dave, U. *Effect of Freeze-Thaw on K-Based Geopolymer Concrete and Portland Cement Concrete*, 6th ed.; Nirma University: Gujarat, India, 2017.
31. Yang, C.; Gupta, R. Prediction of the compressive strength from resonant frequency for low-calcium fly ash-based geopolymer concrete. *J. Mater. Civ. Eng.* **2018**, *19*, 435–533. [[CrossRef](#)]
32. American Society for Testing and Materials. *Standard Practice for Making and Curing Concrete Test Specimens in the Laboratory*; ASTM C192/C192M—15; ASTM: West Conshohocken, PA, USA, 2015.
33. American Society for Testing and Materials. *Standard Test Method for Compressive Strength of Cylindrical Concrete Specimens*; ASTM C39/C39M—15; ASTM: West Conshohocken, PA, USA, 2015.
34. Kumaravel, S. Development of various curing effect of nominal strength Geopolymer concrete. *J. Eng. Sci. Technol. Rev.* **2014**, *7*, 116–119. [[CrossRef](#)]
35. Nath, P.; Sarker, P. Effect of GGBFS on setting, workability and early strength properties of fly ash geopolymer concrete cured at ambient condition. *Constr. Build. Mater.* **2014**, *66*, 163–171. [[CrossRef](#)]
36. Hardjito, D.; Rangan, B. *Development and Properties of Low-Calcium Fly Ash-Based Geopolymer Concrete*; Curtin University of Technology: Perth, Australia, 2005.
37. American Society for Testing and Materials. *Standard Test Method for Resistance of Concrete to Rapid Freezing and Thawing*; ASTM C666; ASTM: West Conshohocken, PA, USA, 2015.
38. Aas-Jalobsen, K. *Fatigue of Concrete Beams and Columns*; Division of Concrete Structure, Norwegian Institute of Technology: Trondheim, Norway, 1970.
39. American Society for Testing and Materials. *Standard Test Method for Slump of Hydraulic-Cement Concrete*; ASTM C143/C143M; American Society for Testing and Materials: West Conshohocken, PA, USA, 2015.
40. Temujin, J.; Williams, R.P.; van Riessen, A. Effect of mechanical activation of fly ash on the properties of geopolymer cured at ambient temperature. *J. Mater. Process. Technol.* **2009**, *209*, 5276–5280. [[CrossRef](#)]
41. Reddy, C.S.; Mohanty, S.; Shaik, R. Physical, chemical and geotechnical characterization of flyash, bottom ash and municipal solid waste from Telangana State in India. *Int. J. GeoEng.* **2018**, *9*, 1–23.
42. Pangdaeng, S.; Phoo-Ngernkham, T.; Sata, V.; Chindaprasirt, P. Influence of curing conditions on properties of high calcium fly ash geopolymer containing Portland cement as additive. *Mater. Des.* **2014**, *53*, 269–275. [[CrossRef](#)]
43. Li, X.; Wang, Z.; Jiao, Z. Influence of curing on the strength development of calcium-containing geopolymer mortar. *Materials* **2013**, *6*, 5069–5076. [[CrossRef](#)]
44. Yewale, V.V.; Shirsath, M.N.; Hake, S.L. Evaluation of efficient type of curing for geopolymer concrete. *Int. J. New Technol. Sci. Eng.* **2016**, *3*, 10–14.
45. Xie, T.; Ozbakkaloglu, T. Behavior of low-calcium fly and bottom ash-based geopolymer concrete. *Ceramic International* **2015**, *41*, 5945–5958. [[CrossRef](#)]
46. Chindaprasirt, P.; Jaturapitakkul, C.; Chalee, W.; Rattanasak, U. Comparative study on the characteristics of fly ash and bottom ash geopolymers. *Waste Manag.* **2009**, *29*, 539–543. [[CrossRef](#)]
47. Hardjito, D.; Fung, S.S. Fly ash-based geopolymer mortar incorporating bottom ash. *Mod. Appl. Sci.* **2010**, *4*, 44. [[CrossRef](#)]
48. Thokchom, S.; Mandal, K.K.; Ghosh, S. Effect of Si/Al ratio on performance of fly ash geopolymers at elevated temperature. *Arab J. Sci. Eng.* **2012**, *37*, 977–989. [[CrossRef](#)]
49. Khale, D.; Chaudhary, R. Mechanism of geopolymerization and factors influencing its development: A review. *J. Mater. Sci.* **2007**, *42*, 729–746. [[CrossRef](#)]
50. Barbosa, V.; MacKenzie, J. Synthesis and thermal behaviour of potassium sialate geopolymers. *Mater. Lett.* **2003**, *57*, 1477–1482. [[CrossRef](#)]

51. Kamseu, E.; Rizzuti, A.; Leonelli, C.; Perera, D. Enhanced thermal stability in K₂O-metakaolin-based geopolymer concretes by Al₂O₃ and SiO₂ fillers addition. *J. Mater. Sci.* **2010**, *45*, 1715–1724. [[CrossRef](#)]
52. Lizcano, M.; Kim, H.S.; Basu, S.; Radovic, M. Mechanical properties of sodium and potassium activated metakaolin-based geopolymers. *J. Mater. Sci.* **2012**, *47*, 2607–2616. [[CrossRef](#)]
53. Hounsi, A.D.; Lecomte-Nana, G.; Djétéli, G.; Blanchart, P.; Alowanou, D.; Kpelou, P.; Napo, K.; Tchangbédji, G.; Praisler, M. How does Na, K alkali metal concentration change the early age structural characteristic of kaolin-based geopolymers. *Ceram. Int.* **2014**, *40*, 8953–8962. [[CrossRef](#)]
54. Nath, P.; Sarker, P.K. Use of OPC to improve setting and early strength properties of low calcium fly ash geopolymer concrete cured at room temperature. *Cem. Concr. Compos.* **2015**, *55*, 205–214. [[CrossRef](#)]
55. Azarsa, P.; Gupta, R. Novel approach to microscopic characterization of cryo formation in air voids of concrete. *Micron* **2019**, *122*, 21–27. [[CrossRef](#)]
56. Mehta, P.K.; Monteiro, P.J. *Concrete Microstructure, Properties, and Materials*, 4th ed.; McGraw-Hill Education: New York, NY, USA, 2014.
57. El-Eswed, B.; Yousef, R.; Alshaaer, M.; Hamadneh, I.; Al-Gharabli, S.; Khalili, F. Stabilization/solidification of heavy metals in kaolin/zeolite based geopolymers. *Int. J. Miner. Process.* **2015**, *137*, 34–42. [[CrossRef](#)]
58. Qian, G.; Sun, D.; Tay, J. Immobilization of mercury and zinc in an alkali-activated slag matrix. *J. Hazard. Mater.* **2003**, *101*, 65–67. [[CrossRef](#)]
59. Ahmari, S.; Zhang, L. Durability and leaching behavior of mine tailings-based geopolymer bricks. *Constr. Build. Mater.* **2013**, *44*, 743–750. [[CrossRef](#)]
60. Nikolic, V.; Komljenovic, M.; Marjanovic, N.; Bascarevic, Z.; Petrovic, R. Lead immobilization by geopolymers based on mechanically activated fly ash. *Ceram. Int.* **2014**, *40*, 8479–8488. [[CrossRef](#)]
61. Izquierdo, M.; Querol, X.; Phillipart, C.; Antenucci, D.; Towler, M. The role of open and closed curing conditions on the leaching properties of fly ash-slag-based geopolymer. *J. Hazard. Mater.* **2010**, *176*, 623–628. [[CrossRef](#)]



© 2020 by the authors. Licensee MDPI, Basel, Switzerland. This article is an open access article distributed under the terms and conditions of the Creative Commons Attribution (CC BY) license (<http://creativecommons.org/licenses/by/4.0/>).